Steel Innovations Conference 2013
Christchurch, New Zealand
21-22 February 2013

DESIGN OF LSF WALL STUDS UNDER FIRE CONDITIONS

S. Gunalan[1] and M. Mahendran[2]

ABSTRACT

Cold-formed steel lipped channels are commonly used in LSF wall construction as load bearing studs with plasterboards on both sides. Under fire conditions, cold-formed thin-walled steel sections heat up quickly resulting in fast reduction in their strength and stiffness. Usually the LSF wall panels are subjected to fire from one side which will cause thermal bowing, neutral axis shift and magnification effects due to the development of non-uniform temperature distributions across the stud. This will induce an additional bending moment in the stud and hence the studs in LSF wall panels should be designed as a beam column considering both the applied axial compression load and the additional bending moment. Traditionally the fire resistance rating of these wall panels is based on approximate prescriptive methods. Very often they are limited to standard wall configurations used by the industry. Therefore a detailed research study is needed to develop fire design rules to predict the failure load and hence the failure time of LSF wall panels subject to non-uniform temperature distributions. This paper presents the details of an investigation to develop suitable fire design rules for LSF wall studs under non-uniform elevated temperature distributions. Applications of the previously developed fire design rules based on AISI design manual and Eurocode 3 Parts 1.2 and 1.3 to LSF wall studs were investigated in detail and new simplified fire design rules based on AS/NZS 4600 and Eurocode 3 Part 1.3 were proposed in the current study with suitable allowances for the interaction effects of compression and bending actions. The accuracy of the proposed fire design rules was verified by using the results from full scale fire tests and extensive numerical studies.

Introduction

Cold-formed steel wall systems are made of light gauge steel frames (see Fig. 1 (a)) lined with gypsum plasterboards. These thin-walled steel studs are subjected to axial compression loads, and are protected by plasterboard linings during fire events as these linings not only delay the rapid temperature rise in steel studs but also provide lateral restraints to them. Since LSF walls are usually exposed to fire attack from one side, the studs are subjected to highly non-uniform elevated temperature distributions during fire events. Such non-uniform temperature distributions will induce complicated structural behaviour of studs involving thermal bowing and magnification effects, non-uniform distribution of strength and stiffness of steel across the cross-section and neutral axis shift (see Figs. 1 (b) and (c)). These effects due to non-uniform temperature distributions cause the thin-walled studs to be subjected to combined axial compression and bending actions during fire events. They compound the already complex structural behaviour of thin-walled steel studs involving local and global buckling effects depending on the level of support provided by plasterboard linings during fires. Therefore it is important that suitable design rules that consider these effects are available to predict the axial compression strength of LSF wall studs and the failure times of LSF walls under standard fire conditions.

Traditionally the fire resistance rating (FRR) of load-bearing LSF wall systems is based on approximate prescriptive methods developed based on limited fire tests. Very often they are limited to standard wall configurations used by the industry. Hence suitable fire design rules were developed for LSF walls subjected to non-uniform temperature distributions by previous researchers. Klippstein (1980) and Gerlich et al. (1996) developed them based on the AISI design manual while Eurocode 3 was used in Ranby (1999), Wang and Davies (2000), Kaitila (2002), Feng and Wang (2005) and Zhao et al. (2005). However, these fire design rules were found to be either inaccurate at times or very complex and hence may not be used in routine fire design of LSF walls (Gunalan 2011). Therefore a detailed research study into the fire performance of LSF

[1]Associate Lecturer, Science and Engineering Faculty, Queensland University of Technology, Brisbane, QLD 4000
[2]Professor, Science and Engineering Faculty, Queensland University of Technology, Brisbane, QLD 4000

wall systems was undertaken to develop improved fire design rules using the results from a series of full scale fire tests and extensive numerical studies.

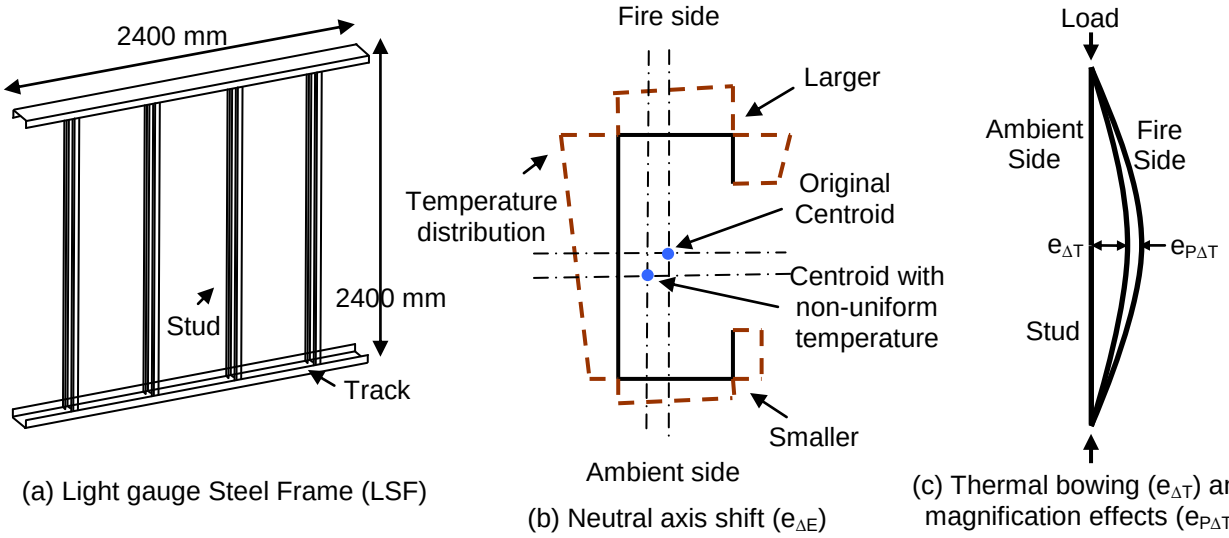

(a) Light gauge Steel Frame (LSF)

(b) Neutral axis shift ($e_{\Delta E}$)

(c) Thermal bowing ($e_{\Delta T}$) and magnification effects ($e_{P\Delta T}$)

Figure 1. The behaviour of LSF wall system in fire

Ten full scale fire tests of load bearing LSF wall assemblies made of eight different wall configurations (Kolarkar 2010), Gunalan 2011 and Gunalan et al. 2013) including a new composite panel were first conducted under standard fire conditions (see Table 1). Numerical studies were then undertaken using suitable LSF wall stud models (Gunalan 2011, Gunalan and Mahendran 2013). The developed finite element models were validated by comparing their results with test results in Kolarkar (2010), Gunalan (2011) and Gunalan et al. (2013). The validated model was then used in a detailed numerical study into the axial compression strength of lipped channel studs used in both the conventional and the new composite panel systems to increase the understanding of their behaviour under non-uniform elevated temperature conditions and to develop fire design rules. The numerical study also included LSF walls made of other steel grades and thicknesses. Since the fire tests showed that the plasterboards provided sufficient lateral restraint until the failure of LSF wall panels, this assumption was also used in the numerical analyses and was further validated by comparison with experimental results. Hence only the flexural buckling of studs about the major axis and local buckling were considered here.

This paper uses the fire performance results of eight different LSF wall systems from fire tests and numerical studies to investigate the previous fire design rules for LSF walls subjected to non-uniform elevated temperatures, and proposes new fire design methods based on AS/NZS 4600 (SA, 2005), AISI S100 (NAS, 2007) and Eurocode 3 Part 1.3 (ECS, 2006). A spread sheet based design tool was developed based on the new design rules to predict the failure load ratio versus time and temperature curves for varying LSF wall configurations shown in Table 1. This paper presents the details and results of this study aimed at developing improved fire design rules for predicting the load capacity of LSF wall studs and the failure times of LSF walls under standard fire conditions. It also includes brief details of the experimental and numerical studies of LSF walls conducted by the authors from which the results were used in this paper.

Experimental Investigation

Ten fire tests of LSF walls were conducted first to evaluate the fire performance of load bearing LSF wall assemblies. One wall specimen was tested to failure under an axial compression load at room temperature while ten wall specimens subjected to a constant axial compression load were exposed to standard fire conditions on one side (see Table 1). Conventional LSF wall assemblies lined with single or double layers of plasterboard with or without cavity insulation were considered. A new LSF wall system based on a composite panel was proposed in which the insulation was placed externally between the two plasterboards (Kolarkar 2010, Gunalan 2011 and Gunalan et al. 2013). The insulations used were glass, rockwool and cellulose fibres. All the steel frames were built to a height of 2400 mm and a width of 2400 mm as shown in Fig. 1 (a). The studs and tracks used in the test frames were fabricated from G500 galvanized steel sheets with a nominal base metal thickness of 1.15 mm. The measured yield strength and elastic modulus of steel were 569 MPa and 213520 MPa, respectively, at ambient temperature. Test frames were lined on both sides by single or double layers of 16 mm gypsum plasterboards. Table 1 shows the details of wall specimens with eight different wall configurations used in this research.

Table 1. Failure times from experiments and FEA

Test	Configuration	Insulation	Load Ratio	Failure Time (min.)	
				Test	FEA
1	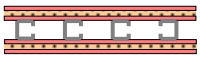	Glass Fibre	0.2	118	115
2	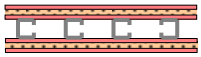	Glass Fibre	0.4	108	110
3	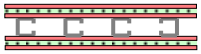	Rock Fibre	0.4	134	131
1*		None	0.2	53	53
2*		None	0.2	111	115
3*	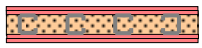	Glass Fibre	0.2	101	100
4*	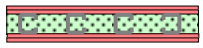	Rock Fibre	0.2	107	105
5*	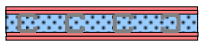	Cellulose Fibre	0.2	110	109
6*	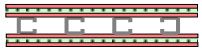	Rock Fibre	0.2	136#	154
7*	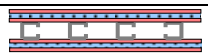	Cellulose Fibre	0.2	124	129

(1 - 3) - Tests conducted by Gunalan (2011); (1* - 7*) - Tests conducted by Kolarkar (2010); (#) - Earlier failure time due to lack of thermal expansion

The furnace was designed to deliver heat based on the standard fire curve as given in AS 1530.4 (SA, 2005). The loading frame was specially designed to load the individual studs of LSF wall specimens in compression from the bottom side using jacks (see Fig. 2 (a)). The axial shortenings of the studs and the out-of-plane movements of the wall specimen were measured using LVDTS while K type thermocouples were used to measure the temperature development across the wall specimens during the fire tests. In each fire test an axial compression load of 15 kN (for a load ratio of about 0.2) or 30 kN (for a load ratio of about 0.4) was applied to each stud, ie. 0.2 or 0.4 times the ultimate capacity of 79 kN of each stud at ambient temperature as obtained from test. The load was held constant at room temperature before the furnace was started and then maintained throughout the fire test. During the fire test, the furnace temperature was regulated to follow the standard temperature-time curve. The test was stopped immediately after one or more of the wall studs failed, and the time to failure (FRR) was recorded. Fig. 2 (b) shows the LSF wall panel and the studs after failure while Table 1 shows their failure times. Further details about the experimental study and test results are given in Kolarkar (2010), Gunalan (2011) and Gunalan et al. (2013).

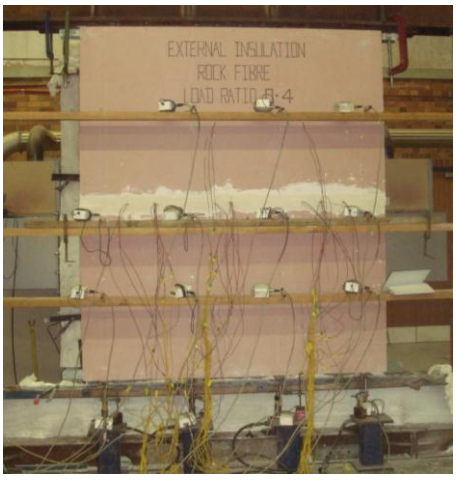

(a) Before the fire test – Ambient side

(b) After the fire test – Fire side

Figure 2. Test Specimen Before and After the Fire Test

Finite Element Modelling

A finite element model of LSF wall studs was developed with appropriate thermal and structural boundary conditions to simulate their behaviour under fire conditions and to determine the FRR. Finite element analyses were conducted under steady state conditions. Here, the non-uniform temperature distributions in the steel stud cross-section were raised to the measured temperatures of hot and cold flanges and web elements at a given time during the standard fire test and then maintained. A load was then applied in increments until the failure of stud. The stud failure load thus obtained was then expressed as a ratio of the ambient temperature stud capacity (load ratio) and plotted against time for each test. The use of steady state analyses provided load ratio versus time curves that can be used to find FRR.

S4R shell element type with a 4 mm x 4 mm mesh size was selected based on detailed convergence studies. The measured mechanical properties were used to enable the comparison of FEA and test results. Poisson's ratio of steel was assumed as 0.3. The yield strength and elastic modulus reduction factors at elevated temperatures and the stress-strain curves were based on the predictive equations developed in Dolamune Kankanamge and Mahendran (2011). The coefficient of thermal expansion α given in Eurocode 3 Part 1.2 (ECS, 2005) was used. Based on other numerical studies (Kaitila 2002, Zhao et al. 2005 and Feng et al. 2003) and the experimental behaviour of studs (Kolarkar 2010, Gunalan 2011 and Gunalan et al. 2013), one of the two central studs with the vertical plasterboard joint against it (critical stud) was considered in the analyses. Pinned support conditions were simulated using rigid plates while the axial compressive load was applied at the section centroid at one end as shown in Fig. 3 (a). It was assumed that the plasterboard on both flanges provided sufficient lateral restraint until failure (Kaitila 2002, Zhao et al. 2005 and Feng et al. 2003). The measured time-temperature profiles obtained from the fire tests were used as was done in Kaitila (2002) and Zhao et al. (2005). The temperatures of the studs were measured at mid-height and quarter points throughout the fire tests. Therefore the average measured temperatures were used over the entire stud length. Non-uniform temperature distribution across the stud (see Fig. 2 (b)) was considered in the finite element modelling of studs. The flange and lip temperatures were assumed to be the same with the web having a linear temperature distribution. The local web buckling near the support was predominant in the first eigen mode of the elastic buckling analyses and also in the test results (Kolarkar 2010 and Gunalan et al. 2013). Therefore this eigen mode was used to introduce the initial geometric imperfection with an amplitude of 0.006b. The effect of residual stress on the ultimate capacity of LSF stud was found to be small at ambient temperature. It will be even more insignificant at elevated temperatures. Hence residual stresses were not considered for studs under fire conditions (Kaitila 2002, Zhao et al. 2005 and Feng et al. 2003).

The results from finite strip analyses (CUFSM) and tests (Kolarkar 2010 and Gunalan 2011) were used to validate the results of finite element analyses (FEA) at ambient temperature. Under fire conditions, many steady state analyses conducted in close time intervals led to a load ratio versus time curve for the LSF wall systems in Table 1. Fig. 3 (b) shows this curve for the case of LSF wall with glass fibre external insulation. As shown in these figures, the failure time for Test 1 with a load ratio of 0.2 were obtained as 115 minutes. The main advantage of steady state FEA is that the figures such as Fig. 3 (b) can now be used to obtain the fire resistance rating (failure time) for any given load ratio. Table 1 gives the failure times predicted by steady state FEA for all the tests. These comparisons show that the developed finite element model accurately predicts the ultimate capacities and failure modes of studs subjected to axial compression under fire conditions. The developed finite element models were able to predict the failure times within 5 minutes. Further details of numerical studies can be found in Gunalan (2011) and Gunalan and Mahendran (2013).

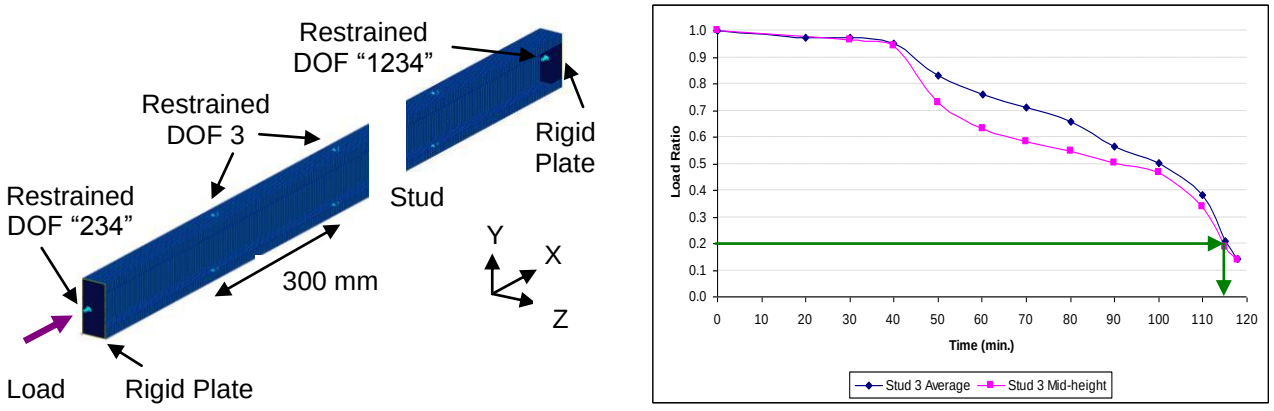

(a) Loading and boundary conditions (b) Load ratio versus Time

Figure 3. Details of finite element modelling

Proposed Fire Design Rules based on Eurocode 3 Part 1.3

Design rules to find the ultimate capacity of LSF wall studs during standard fires were developed by Ranby (1999), Wang and Davies (2000), Kaitila (2002), Feng and Wang (2005) and Zhao et al. (2005) using Eurocode 3 Parts 1.2 and 1.3. A detailed review of the design rules proposed by them in relation to the applicability to LSF wall studs is given in Gunalan (2011). Among them, Feng and Wang's (2005) proposals based on Eurocode 3 Part 1.3 design rules for ambient temperature conditions agreed well with the FEA and fire test results from this study. Therefore this study is also based on Eurocode 3 Part 1.3 to develop simplified fire design rules. Among the previous studies except Feng and Wang (2005), the minor axis bending was not considered. This is due to the availability of plasterboard restraint. Feng and Wang (2005) included the neutral axis shift about the minor axis and corresponding bending moment. However, they showed that this effect is negligible and can be ignored in the fire design of LSF wall studs. Therefore the relevant equation in Eurocode 3 Part 1.3 for the combined actions of bending and axial compression can be reduced to,

$$\frac{N_{Ed}}{\chi_x f_y A_{eff} / \gamma_{M1}} + \frac{k_{xx}\left(M_{x,Ed} + \Delta M_{x,Ed}\right)}{\chi_{LT} f_y W_{eff,x} / \gamma_{M1}} = 1 \quad (1)$$

where N_{Ed} is the applied axial compression load and f_y is the basic yield strength; A_{eff} is the effective cross-sectional area for axial compression; γ_{M1} is the partial factor for resistance of members to instability which was assumed to be equal to 1; $M_{x,Ed}$ is the applied bending moment about the major axis; $\Delta M_{x,Ed}$ is the additional moment; $W_{eff,x}$ is the effective section modulus for the maximum compressive stress in an effective cross-section that is subject to bending about the major axis; χ_x and χ_{LT} are the reduction factors due to flexural buckling and lateral torsional buckling and k_{xx} is the interaction factor.

The bending moment about the major axis is caused by three effects due to the non-uniform temperature distribution in LSF wall studs. They are the pure thermal bowing, the neutral axis shift due to the deterioration of stiffness and the magnification effects due to P-Δ effects. If the net eccentricity of these three effects is denoted as "e", the bending moment about the major axis is $N_{Ed}\, e$. For members not susceptible to torsional deformations such as LSF wall studs, χ_{LT} is equal to 1.0. In Eq. 1, the component $f_y A_{eff}$ is the ultimate failure load for local buckling N_{eff} and the component $f_y W_{eff,x}$ is the section moment capacity $M_{x,eff}$ of LSF wall stud. Hence the common equation used by all the previous researches (Ranby 1999, Wang and Davies 2000, Kaitila 2002, Feng and Wang 2005 and Zhao et al. 2005) is

$$\frac{N_{Ed}}{\chi_x N_{eff}} + \frac{k_{xx} N_{Ed} e}{M_{x,eff}} = 1 \quad (2)$$

In order to find the ultimate load N_{Ed} of LSF wall studs under standard fire conditions, the parameters k_{xx}, e, χ_x, N_{eff} and $M_{x,eff}$ should be determined accurately by taking into account the effects of non-uniform elevated temperature distribution in LSF wall studs. The calculation methods of these parameters and assumptions varied in the previous studies and hence different ultimate loads were obtained for LSF wall studs.

Section Compression Capacities of LSF Wall Studs under Fire Conditions (N_{eff})

The local buckling capacity according to Eurocode 3 Part 1.3 was calculated by multiplying the effective area and the yield stress at elevated temperatures. Three possible yield stresses were investigated by Gunalan (2011): yield stress at the average stud (web) temperature ($f_{y,web}$), area based weighted average yield stress of the gross section ($f_{y,bar}$) and yield stress at hot flange temperature ($f_{y,HF}$). Similarly four different effective areas were investigated: effective area at ambient (A_{20}), elevated (A_t), web (A_w) and hot flange (A_{HF}) temperatures. Hence the local buckling capacities were predicted for 12 different cases (four effective areas x three yield stresses) using the relevant design rules in Eurocode 3 Part 1.3. Three options were short listed among them to find the local buckling capacity of LSF wall studs with non-uniform temperature distributions ($f_{y,bar}$ with A_t, A_w and A_{20}). At higher load ratios the load ratio curve using the effective areas at elevated temperatures (A_t) agreed well with FEA results compared to the load ratio curve using A_{20}. However, at lower load ratios none of them agreed with FEA results. In FEA, the entire hot flange has reached its yield strength capacity at failure time and triggered the failure. However, at this time the cold flange has not reached its yield strength. This indicates that the cold flange has some reserve capacity at the time the stud failed. However, in the prediction of local buckling capacity at elevated temperatures according to $\Sigma A_i f_{yi}$, it is assumed that the entire stud cross-section has reached its yield stress. This resulted in the over-estimation of local buckling capacity of studs with non-uniform temperature distributions. Therefore it was decided to

limit the yield stress of cold flange to 1.5 f_{yHF} in the determination of local buckling capacity. This indicated a better agreement in load ratios with FEA results (Gunalan 2011).

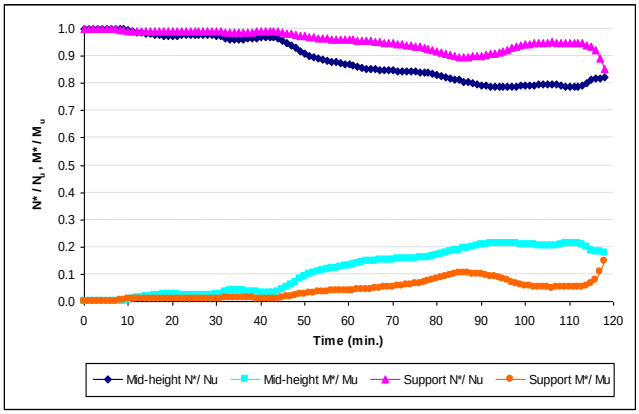

Figure 4. Interaction of compression and bending for Test 1

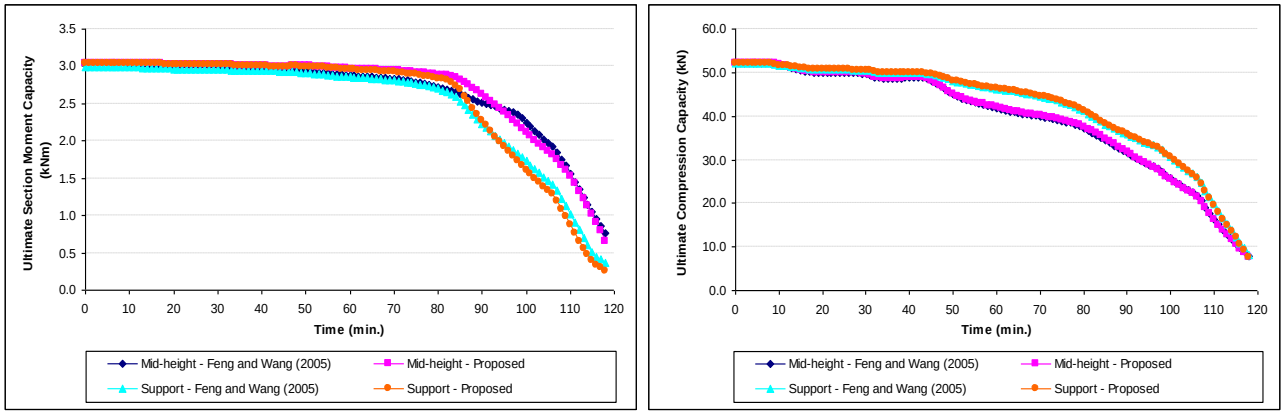

(a) Section moment capacity (b) Ultimate compression capacity

Figure 5. Ultimate compression and section moment capacities versus time for Test 1

Member Compression Capacities of LSF Wall Studs under Fire Conditions ($\chi_x N_{eff}$)

Ranby (1999) and Kaitila (2002) used the mechanical properties at average stud (web) temperatures to find the member compression capacities of LSF wall studs subjected to non-uniform temperature distributions. However, Feng and Wang (2005) and Zhao et al. (2005) used the weighted average mechanical properties based on gross section dimensions. It was found that the weighted average mechanical properties should be used instead of the mechanical properties at web temperature (Gunalan 2011). Hence in this study the weighted average mechanical properties were used with Eurocode 3 Part 1.3 design rules to determine the member compression capacities of LSF wall studs under fire conditions.

Section Moment Capacities of LSF Wall Studs under Fire Conditions ($M_{x,eff}$)

Ranby (1999) and Kaitila (2002) used the basic formula $f_{y,web}Z_{eff,20}$ to find the section moment capacities of LSF wall studs subject to non-uniform temperature distributions. They used the yield stress at web temperature and the effective section modulus at ambient temperature. The section modulus was calculated based on the effective element widths for pure compression. However, it is important that the effective element widths based on pure bending are used. Feng and Wang (2005) suggested a more accurate method to find the section moment capacity. When calculating $M_{x,eff}$ at stud mid-height, compression is on the cold flange side with a high yield strength and tension is on the hot side with a low yield strength. In this case partial plasticity was considered whereby tensile stress in the extreme fibres has reached yield and the maximum compression stress in the extreme fibre is equal to the yield stress. At the supports since the hot flange is in compression, the first yield of compression flange was adopted. Zhao et al.'s (2005) assumption was similar to that proposed in Feng and Wang (2005).

Fig. 4 shows the interaction of compression and bending in Test 1 using the ratio of applied axial compression load and axial compression capacity (N^*/N_u) and the ratio of applied bending moment and

section moment capacity (M^*/M_u). The influence of bending is high at mid-height compared at the support. However, overall, this figure clearly indicates that the LSF wall studs under non-uniform temperature distributions are dominated by compression than bending. Therefore it was decided to propose a simplified method to calculate the section moment capacity. It is proposed here that the section moment capacity at mid-height is calculated using the formula $f_{y,bar}Z_{eff,t}$ where $f_{y,bar}$ is the area based weighted average yield stress and $Z_{eff,t}$ is equal to $I_{eff,t} / y_{max}$. In the studies of Feng and Wang (2005) and Zhao et al. (2005), partial plasticity was considered at mid-height whereby tensile stress in the extreme fibres has reached yield and the maximum compression stress in the extreme fibre is equal to the yield stress. Therefore in this scenario f_{ybar} is suitable to calculate the section moment capacity. $I_{eff,t}$ is the weighted average second moment of area (taking into account the variation of elastic modulus with temperature across the section) calculated based on the effective element widths at elevated temperatures. The effective area for pure bending was calculated assuming compression on cold flange.

In the studies of Feng and Wang (2005) and Zhao et al. (2005), the moment capacity at the support was calculated with yielding occurring in the hot flange. In this case $f_{y,HF}$ is suitable to calculate the section moment capacity instead of $f_{y,bar}$. Therefore it is proposed to calculate the section moment capacity at support using the formula $f_{y,HF}Z_{eff,t}$. This time the effective area for pure bending should be calculated assuming compression on hot flange. This will introduce additional calculation effort without improving the accuracy much and hence not proposed in the current study. Therefore the effective area used in the mid-height calculations (assuming compression on cold flange) is also recommended for support calculations.

Fig. 5 (a) shows the variation of section moment capacity ($M_{x,eff}$) with time for Test 1 according to Feng and Wang (2005) and the current simplified proposal for both mid-height and supports. A reasonable agreement was achieved between the accurate method of Feng and Wang (2005) and the proposed simplified method in this section. Fig. 5 (b) shows the variation of ultimate compression capacities (N_{Ed}) of LSF wall studs with time at mid-height and supports for the same tests. It shows that the ultimate compression capacities were not affected by using the simplified method for section moment capacities. This is due to the fact that the LSF wall studs subjected to non-uniform temperature distributions are dominated by compression rather than bending as shown in Fig. 4. Therefore it is concluded that the section moment capacities can be calculated using the simplified method proposed here without affecting the accuracy of ultimate compression capacities of LSF wall studs.

Interaction of Compression and Bending

The effect of thermal bowing can be considered as that of an initial geometric imperfection of a slender member with pinned ends. Hence the bending moment generated by thermal bowing and its magnification effect is given by,

$$N_{Ed}e_1 = \frac{N_{Ed}e_{\Delta T}}{1-\frac{N_{Ed}}{N_{cr}}} \qquad \text{with} \qquad e_{\Delta T} = \frac{\alpha L^2 \delta T}{8b_w} \tag{3}$$

where N_{Ed} is the applied load; e_1 is the maximum total deformation at mid-height due to thermal bowing and its magnification effects; N_{cr} is the Euler buckling load; $e_{\Delta T}$ is the thermal bowing at mid-height (Cooke 1987); α is the thermal expansion coefficient for steel; L and b_w are the stud height and web depth, respectively, and δ_T is the temperature difference.

Using Eurocode 3 Part 1.3 the bending moment due to the shift of neutral axis about the major axis and its magnification effects is given by Eq. 4 assuming the LSF wall stud is not susceptible to torsional deformation,

$$N_{Ed}e_2 = k_{xx}N_{Ed}e_{\Delta E} \qquad \text{with} \qquad e_{\Delta E} = \frac{\sum_i E_{i,\theta}y_i A_i}{\sum_i E_{i,\theta}A_i} \qquad \text{and} \qquad k_{xx} = \frac{C_{mx}}{1-\chi_x\frac{N_{Ed}}{N_{cr}}} \tag{4}$$

where C_{mx} allows for the effects of non-uniform distribution and applied axial compression load (Eurocode 3 Part 1.3). Since the moment due to neutral axis shift is equal at both ends, $\Psi = 1$ should be used in the determination of C_{mx}. Therefore the total moment due to thermal bowing, neutral axis shift and their magnification effects can be calculated as,

$$M_{x,Ed,tot} = N_{Ed}(e_1 - e_2) = \frac{N_{Ed} e_{\Delta T}}{1 - \frac{N_{Ed}}{N_{cr}}} - \frac{N_{Ed} e_{\Delta E} C_{mx}}{1 - \chi_x \frac{N_{Ed}}{N_{cr}}} \quad (5)$$

In the studies of Ranby (1999) and Kaitila (2002), the magnification effects were counted twice by the use of Eq. 3 and k_{xx}. This is not recommended in the fire design of LSF wall studs and hence the proposed method in this section should be used. In this study, the equations given in Eurocode 3 Part 1.3 are reduced to Eq. 6 to obtain the ultimate compression capacities (N_{Ed}) of LSF wall studs subjected to non-uniform temperature distributions.

$$\frac{N_{Ed}}{\chi_x N_{eff}} + \frac{M_{x,Ed,tot}}{M_{x,eff}} = 1 \quad (6)$$

where N_{eff}, χ_x, $M_{x,eff}$ and $M_{x,Ed,tot}$ are obtained as discussed before.

Proposed Fire Design Rules based on AS/NZS 4600 and AISI S100

Klippstein (1980) and Gerlich et al. (1996) developed fire design rules for LSF wall studs using the AISI design manual. Fire design calculations based on their rules can be found in Gunalan (2011). The equations used by Klippstein (1980) are not available in the current AISI S100 document (AISI, 2007). Gerlich et al. (1996) calculated the critical stress and the bending moment capacity based on the yield stress at cold flange temperature. This resulted in the over-estimation of failure times of LSF wall panels. In this section suitable fire design rules are proposed based on the ambient temperature cold-formed steel design codes (AS/NZS 4600 and AISI S100) that have identical design rules. As discussed before, Eq. 7 is proposed here to obtain the ultimate compression capacities of LSF wall studs subjected to non-uniform temperature distributions. It is based on Eq. 6 but rewritten using the symbols in AS/NZS 4600 and AISI S100.

$$\frac{N^*}{A_{eff,t} f_n} + \frac{M^*}{M_{x,eff}} = 1 \quad (7)$$

where N^* and M^* are the applied axial compression load and the total moment about the major axis; f_n is calculated based on the weighted average mechanical properties (yield stress and elastic modulus) at elevated temperatures and includes the effects of major axis flexural buckling; $A_{eff,t}$ is the effective area at elevated temperature calculated using f_n; The determination of member compression capacity using AS/NZS 4600 is much simpler than using Eurocode 3 Part 1.3, since the Australian design code finds the member capacity directly using f_n rather than finding it from the section capacity as was done in European design code. $M_{x,eff}$ is the section moment capacity calculated as before.

The total moment M^* due to thermal bowing, neutral axis shift and their magnification effects is given by

$$M^* = \frac{C_{mx} N^* e}{\alpha_{nx}} = \frac{N^* e_{\Delta T}}{1 - \frac{N^*}{N_{cr}}} - \frac{N^* e_{\Delta E}}{1 - \frac{N^*}{N_{cr}}} \quad (8)$$

where C_{mx} is equal to 1 in the case of neutral axis shift as the moments developed in this case is uniform.

Detailed calculations to find the ultimate capacity of LSF wall studs at elevated temperatures based on AS/NZS 4600 (SA, 2005) and Eurocode 3 Part 1.3 (ECS, 2006) design rules are given in Gunalan (2011).

Comparison of Proposed Fire Design Rules with Test and FEA Results

Fig. 6 compares the variation of FEA load ratios with predicted load ratios based on Australian and European codes (AS/NZS 4600 and Eurocode 3 Part 1.3). A reasonable agreement was obtained between the FEA results and the predictions. A very good agreement was obtained between AS/NZS 4600 and Eurocode 3 Part 1.3 although the latter is slightly conservative in predicting the failure times for lower load ratios. Table 2 compares the test and FEA results with the predicted failure times (FRR) using the proposed fire design

rules based on AS/NZS 4600 and Eurocode 3 Part 1.3, respectively. The agreement is very good and it is concluded that the proposed fire design rules using AS/NZS 4600 and Eurocode 3 Part 1.3 accurately predict the failure times of LSF wall panels subject to fire from one side.

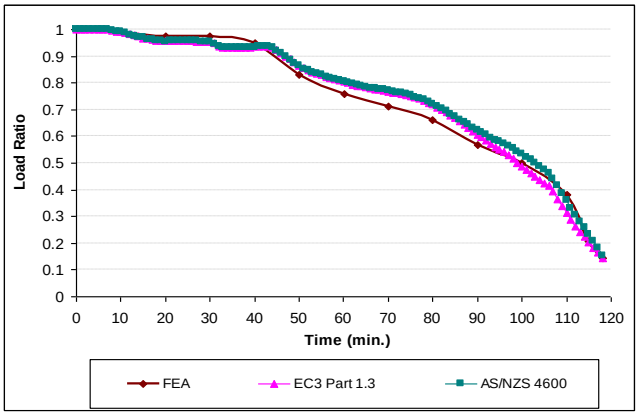

Figure 6. Comparison of proposed fire design rules with FEA results for Test 1

Table 2. Failure times predicted by the proposed fire design rules

Test	Load Ratio = 0.2				Load Ratio = 0.4				Load Ratio = 0.7		
	Test	FEA	AS.	EC3	Test	FEA	AS	EC3	FEA	AS	EC3
1	118	115	117	115	-	109	109	107	72	82	82
2	-	116	116	115	108	110	111	109	85	92	92
3	-	143	137	137	134	131	132	128	95	101	101
1*	53	53	56	53	-	42	44	41	20	25	25
2*	111	115	116	114	-	107	108	105	63	73	73
3*	101	100	97	98	-	88	91	89	62	67	67
4*	107	105	101	101	-	91	94	91	64	67	68
5*	110	109	108	108	-	101	103	102	64	70	70
6*	136[#]	154	155	153	-	137	138	133	99	105	105
7*	124	129	130	128	-	119	119	116	87	93	93

AS and EC3 – Proposed fire design rules using AS/NZS 4600 (2005) and Eurocode 3 Part 1.3 (2006), respectively.

Conclusions

This paper has presented the details of an investigation on the development of suitable fire design rules for LSF walls under standard fire conditions. The behaviour and capacity of LSF wall studs subjected to non-uniform elevated temperature conditions during standard fires was evaluated in detail based on a series of full scale fire tests and extensive numerical studies and comparison with previous fire design rules developed based on American, Australian and European design codes. New simplified fire design rules were proposed based on AS/NZS 4600, AISI S100 and Eurocode 3 Part 1.3 with suitable allowances for the interaction effects of compression and bending actions and the effects of thermal bowing, neutral axis shift and their magnification effects. The accuracy of the proposed fire design rules was verified with the available test and FEA results for LSF wall systems made of eight different wall configurations. The agreement of failure times was very good compared to the complexity and assumptions involved in the fire deign of LSF wall studs.

References

Alfawakhiri, F., 2001, Behaviour of cold-formed-steel-framed walls and floors in standard fire resistance tests, *Ph.D. Thesis*. Carleton University, Ottawa, Canada.

American Iron and Steel Institute (AISI), 2007, *Specifications for the Cold-formed Steel Structural Members, Cold-formed Steel Design Manual*, Washington, USA.

Cooke, G.M.E., 1987, Thermal bowing and how it affects the design of fire separating construction, Fire Research Station, Building Research Establishment, Herts, UK.

Dolamune Kankanamge, N. and Mahendran, M., 2011, Mechanical properties of cold-formed steels at elevated temperatures, *Thin-Walled Structures*, 49, 26-44.

European Committee for Standardization (ECS), *EN 1993-1-2, 2005, Eurocode 3: Design of Steel Structures. Part 1.2: General Rules - Structural Fire Design*, Brussels.

European Committee for Standardization (ECS), *EN 1993-1-3, 2006, Eurocode 3: Design of Steel Structures. Part 1.3: General Rules - Supplementary Rules for Cold-formed Members and Sheeting*, Brussels.

Feng, M., Wang, Y.C. and Davies, J.M., 2003, Axial strength of cold-formed thin-walled steel channels under non-uniform temperatures in fire, *Fire Safety Journal*, 38, 679-707.

Feng, M. and Wang, Y.C., 2005, An analysis of the structural behaviour of axially loaded full-scale cold-formed thin-walled steel structural panels tested under fire conditions, *Thin-Walled Structures*, 43, 291-332.

Gunalan, S., 2011, Structural behaviour and design of cold-formed steel wall systems under fire conditions, *Ph.D. Thesis*, Queensland University of Technology, Brisbane, Australia.

Gunalan, S., Kolarkar, P.N. and Mahendran,, M. 2013, Experimental study of load bearing cold-formed steel wall systems under fire conditions, *Thin-Walled Structures*, Accepted.

Gunalan, S. and Mahendran, M., 2013, Finite element modelling of load bearing cold-formed steel wall systems under fire conditions, *Engineering Structures*, Accepted.

Gerlich, J.T., Collier, P.C.R. and Buchanan, A.H., 1996, Design of steel-framed walls for fire resistance, *Fire and Materials*, 20 (2) 79-96.

Kaitila, O., 2002, Finite element modelling of cold-formed steel members at high temperatures, *Licentiate Thesis*, Laboratory of Steel Structures, Helsinki University of Technology, Espoo, Finland.

Klippstein, K.H., 1980, Strength of cold-formed studs exposed to fire, American Iron and Steel Institute, Washington DC, USA.

Kolarkar, P.N., 2010, Structural and thermal performance of cold-formed steel stud wall systems under fire conditions, *Ph.D. Thesis*, Queensland University of Technology, Brisbane, Australia.

Ranby, A., 1999, Structural fire design of thin-walled steel sections, *Licentiate Thesis*, Lulea University of Technology, Stockholm, Sweden.

Standards Australia (SA), 2005, *AS/NZS 4600*, *Cold-formed Steel Structures*, Sydney, Australia.

Standards Australia (SA), 2005, *AS 1530.4*, *Methods for Fire Tests on Building Materials, Components and Structures Part 4,* Sydney, Australia.

Wang, Y.C. and Davies, J.M., 2000, Design of thin-walled steel channel columns in fire using Eurocode 3 Part 1.3, *Proceeding of the First International Workshop on Structures in Fire*, Copenhagen, 181–193.

Zhao, B., Kruppa, J., Renaud, C., O'Connor, M., Mecozzi, E., Apiazu,. W., Demarco, T., Karlstrom, P., Jumppanen, U., Kaitila, O., Oksanen, T. and Salmi, P., 2005, Calculation rules of lightweight steel sections in fire situations, *Technical Steel Research*, European Union.